DOI: 10.25092/baunfbed.363772 *J. BAUN Inst. Sci. Technol., 19(3) Special Issue, 89-104, (2017)*

Synthesis, spectral characterization, theoretical analysis and antioxidant activities of aldol derivative isophorone structures

Serpil ERYILMAZ[1,*], Melek GÜL[2], Ersin İNKAYA[3]

[1]*Amasya University, Faculty of Arts and Sciences, Department of Physics, Amasya*
[2]*Amasya University, Faculty of Arts and Sciences, Department of Chemistry, Amasya*
[3]*Amasya University, Central Research Laboratory, Amasya*

Geliş Tarihi (Recived Date): 20.08.2017
Kabul Tarihi (Accepted Date): 17.11.2017

Abstract

In this study, the structural properties of isophorone derivatives with π-conjugation obtained by aldol reactions have characterized by spectral analyses such as FT-IR, ^{1}H-NMR, and ^{13}C-NMR. The compounds have optimized using Density Functional Theory (DFT/B3LYP) method with 6-311G(d,p) basis set in the ground state and the geometric parameters have compared with the results obtained by X-ray Single Crystal diffraction technique. Also, the spectral results have examined along with calculated vibrational frequencies, ^{1}H-NMR, ^{13}C-NMR chemical shift values. To get information about the chemical stability of the compounds, some of the structure parameters (ionization potential, electron affinity, electronegativity, chemical hardness-softness, etc.) have been studied at the same theoretical level. Also, NLO properties and antioxidant activities of the compounds have investigated by using DPPH free radical scavenging, reducing power and metal chelating methods. Spectral and theoretical results are compatible with each other.

Keywords: *Isophorone, spectral analysis, DFT, antioxidant activity.*

Aldol türevi izoforan yapılarının sentezi, spektral karakterizasyonu, teorik analizi ve antioksidan aktiviteleri

Özet

Bu çalışmada, aldol tepkimeleri ile elde edilen π konjugasyonuna sahip izoforan türevlerinin yapısal özellikleri FT-IR, ^{1}H-NMR ve ^{13}C-NMR gibi spektral analizler ile karakterize edilmiştir. Yoğunluk Fonksiyoneli Teorisi (YFT/B3LYP) kullanılarak 6-311G(d,p) baz seti ile taban durumunda optimize edilmiş ve geometrik parametreleri, X-ışını Tek Kristal difraksiyon yöntemi ile gerçekleştirilen kristal yapı analizinin sonuçları ile karşılaştırılmıştır. Ayrıca spektral sonuçlar, teorik olarak hesaplanan titreşim frekansları, ^{1}H-NMR ve ^{13}C-NMR kimyasal kayma değerleri ile birlikte incelenmiştir. Bileşiklerin kimyasal kararlılığı hakkında bilgi sahibi olabilmek için bir takım yapı parametreleri (iyonlaşma potansiyeli, elektron ilgisi, elektronegatiflik, kimyasal sertlik-yumuşaklık, v.b.) kuramsal düzeyde incelenmiştir. Bileşiklerin NLO özellikleri ve antioksidan aktiviteleri; DPPH serbest radikal giderme, indirgeme gücü ve metal şelatlama metotları kullanılarak incelenmiştir. Spektral ve kuramsal sonuçlar birbiriyle uyumludur.

Anahtar Kelimeler: *İzoforan, spektral analiz, YFT, antioksidan aktivite.*

[*] Serpil ERYILMAZ, srpleryilmaz@gmail.com, http://orcid.org/0000-0002-0935-4644
Melek GÜL, melekgul2005@yahoo.com, http://orcid.org/0000-0002-0037-1202
Ersin İNKAYA, e_inkaya@hotmail.com, http://orcid.org/0000-0002-8600-7259

1. Introduction

Isophorone has a peppermint-like odour and used as an intermediate component in the organic synthesis and also solvent in the production of paints and printing inks, lacquers, adhesives, resins, waxes, oils, and pesticides [1-4]. Besides the industrial uses of isophorones, are observed to exist environmental water, drinking water and in some nutrients such as cranberries, wheat, rice, beans, soy sauce, etc, [1, 5-7]. Studies on the effects directly affecting human life have reported skin, eye, nose and throat irritations caused by solvent vapour fumes during use in the printing industry [1]. It has also been observed that the studies on animals have caused respiratory failure, allergic contact dermatitis, renal and liver damage [2, 8-11].

Isophorone, α,β-unsaturated carbonyl compound and give aldol reactions with aromatic aldehydes. Aldol reactions are one of the reactions that lead to the formation of significant carbon-carbon bonds in organic synthesis [12]. Also, α,β-unsaturated carbonyl moiety a structural part of the natural product, which has active role of the biological activity such as microbiological reduction [13], anticancer drug [14] etc.

In this paper, our aim is the determination of optimal reaction conditions under microwave, sonication, and conventional methods and investigates the structural properties of naphthyl and chlorophenyl derivatives of isophorone. We have reported that the synthesis process, single crystal X-ray structure, IR and NMR spectral analysis results of the *(E)-5,5-dimethyl-3-(2-(naphyhalen-1-yl)vinyl)-cyclohex-2-enone* and *(E)-3-(4-chlorostyryl)-5,5-dimethylcyclohex-2-enone* compounds. In addition, theoretical analyses on the structures were carried out by using Density Functional Theory (DFT) and evaluated along with experimental results of the molecular geometry parameters, vibrational frequencies, and chemical shifts values. To learn about the chemical reactivity properties of the compounds, frontier molecular orbital energies, ionization potential, electron affinity, electronegativity, chemical hardness-softness etc. electronic structure parameters were examined at the same theoretical level and in the gas phase. In addition to, nonlinear optical (NLO) behaviour and antioxidant activities via DPPH radical scavenging, reducing and metal chelating of compounds were investigated.

2. Experimental details

2.1. Synthesis

The compounds were synthesized by different three methods; conventional thermal, microwave, sonication.

Conventional thermal: 3,5,5-trimethylcyclohex-2-enone (1.1 mmol) was added to aromatic aldehydes (1.1 mmol). The aqueous methanolic sodium hydroxide solutions were added dropwise over 30 minutes. The reaction mixture was refluxed for 12 h, before it was poured into ice-cold water and then left to cool to room temperature. The solid was collected and recrystallized from ethanol.

Microwave: 3,5,5-trimethylcyclohex-2-enone (1.1 mmol), aromatic aldehydes (1.1 mmol) and methanolic sodium hydroxide solutions were placed into the microwave vessel (30 mL), which the vessel was sealed with a pressure control cap, and irradiated 15 min at 400 W. After reaction completion was done same way conventional method.

Sonication: 3,5,5-trimethylcyclohex-2-enone (1.1 mmol) was added to aromatic aldehydes (1.1 mmol). The aqueous methanolic sodium hydroxide solutions were added drop-wise over 30 minutes under N_2 atm. via ultrasound irradiation at 35-40 °C for 6 h. The reaction mixture was terminated and purified similar way of conventional methods.

The synthesis process of the compound **I** (*(E)-5,5-dimethyl-3-(2-(naphyhalen-1-yl)vinyl)-cyclohex-2-enone*) and **II** (*(E)-3-(4-chlorostyryl)-5,5-dimethylcyclohex-2-enone*) which synthesized from 3,5,5-trimethylcyclohex-2-enone and related aldehyde through aldol reaction are shown in Figure 1.

*Compound **I***: *(E)-5,5-dimethyl-3-(2-(naphyhalen-1-yl)vinyl)-cyclohex-2-enone*: White powder; yield % 78, mp 172^{o}C, Rf 0.072 (1:2 Ethylacetate: hexane); FTIR: 3054, 3027, 2964, 1646, 1606, 1578, 1455, 1361, 1301, 1247, 967, 792, 768 cm^{-1}, ^{1}H NMR (600 MHz, $CDCl_3$) δ 8.15 (d, *J* = 8.3 Hz, 1H), 7.86 (dd, *J* = 20.0, 8.0 Hz, 1H), 7.78 (d, *J* = 15.9 Hz, 1H), 7.74 (d, *J* = 6.9 Hz, 1H), 7.63 – 7.44 (m, 1H), 6.97 (d, *J* = 15.9 Hz, 1H), 6.97 (d, *J* = 15.9 Hz, 1H), 6.13 (s, 1H), 2.59 (s, 1H), 2.35 (s, 1H), 1.16 (s, 1H) ppm, ^{13}C NMR (151 MHz, $CDCl_3$) δ 200.19, 154.69, 133.72, 133.39, 132.37, 131.63, 131.24, 129.40, 128.83, 127.36, 126.52, 126.07, 125.63, 124.30, 123.20, 51.47, 39.25, 33.40, 28.58 ppm. LC- MSD: (M^{+}) 276.15, $(M+1)^{+}$ 277.16 m/z.

*Compound **II***: *(E)-3-(4-chlorostyryl)-5,5-dimethylcyclohex-2-enone*: White powder; yield % 80, mp 168^{o}C, Rf 0.081 (1:2 Ethylacetate: hexane); FTIR: 3035, 3027, 2951, 2880, 1655, 1616, 1579, 1486, 1367, 1297, 1243, 968, 836, 828 cm^{-1}, ^{1}H NMR (600 MHz, $CDCl_3$) δ 7.42 (d, *J* = 8.6 Hz, 1H),

7.34 (d, *J* = 8.5 Hz, 1H), 6.91 (q, *J* = 16.2 Hz, 1H), 6.08 (s, 1H), 2.46 (s, 1H), 2.27 (s, 1H), 1.11 (s, 1H) ppm, ^{13}C NMR (151 MHz, $CDCl_3$) δ 200.06, 154.22, 134.75, 134.49, 133.48, 130.13, 129.06, 128.90, 128.34, 127.46, 51.40, 39.02, 33.32, 28.48 ppm. LC-MSD: (M^+) 260.10, $(M+1)^+$ 262.06 m/z.

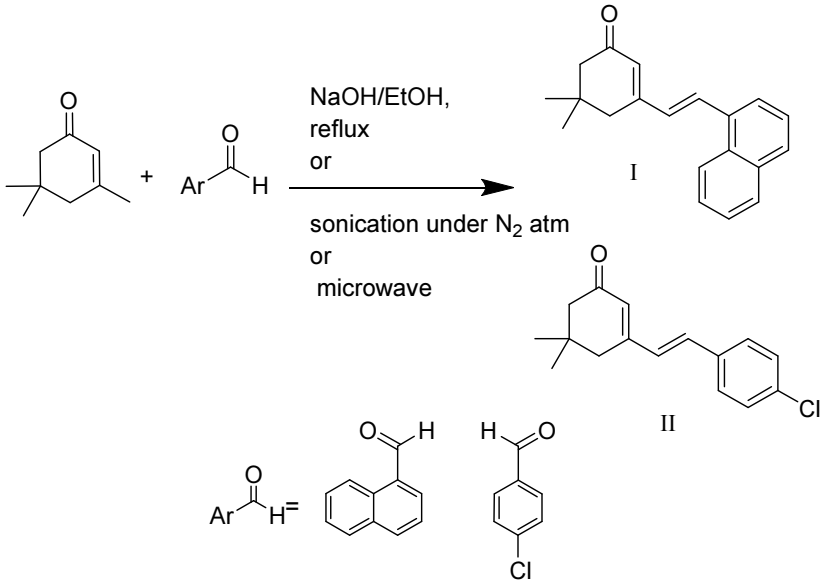

Figure 1. The scheme of the synthesis process of the compounds.

2.2. Materials and instrumentation

Microwave reactions were run using a Discover Synthesis Model of the CEM. Ultrasound assisted reactions were carried out using a Bandelin ultrasound with 35 kHz frequency. IR spectra was obtained with a "Perkin Elmer, FT-IR" system and reported in terms of frequency of absorption (cm^{-1}). Melting point was determined on a capillary point apparatus equipped with digital thermometer, "Thermo". NMR spectra were determined with a "Bruker Ac-400 and 600 MHz NMR". Mass spectrometer was measured with AB-Sciex LC-MS/MS-QTrap. The compounds have been identified in the AUMAULAB Central Laboratory in Amasya University in Turkey.

2.3. Crystallography

The single-crystal X-ray data of the compound I and II were collected on a Bruker D8 QUEST diffractometer. All diffraction measurements were carried out at room temperature (296 K) using graphite monochromated Mo-Kα radiation (λ=0.71073 Å). Reflection data were recorded in the rotation mode with the ω scan technique by using X-AREA software [15]. The structure of cyclohexenone was solved by direct methods using SHELXS-97 [16] and refined by full-matrix least squares techniques against F^2using SHELXL-2014/7 [17] implemented in WinGX [18] program suit. The molecular graphics were done using ORTEP-3 for Windows [18]. The parameters of the refinement process and details of the data collection conditions are given in Table 1.

3. Theoretical analysis details

The theoretical analyses were carried out using the Gaussian 09W [19] package and GaussView 5.0 [20] graphical interface programs for isophorone derivatives compound **I** and **II**. The initial molecular geometries of the compound **I** and **II** were taken on the coordinates obtained from the X-ray diffraction data and the optimization process was carried out using DFT/B3LYP (Becke's Three-Parameter Hybrid Functional using the Lee, Yang and Parr Correlation Functional) [21-23] method with 6-311G(d,p) the basis set in the ground state. Harmonic vibrational frequencies which are helpful in determining the functional groups of the compounds were examined. Because of the spectral values gave anharmonic vibrations [24], the calculated values were multiplied by the scale 0.9682 [25] in order to remove the systematic errors that may occur. ^{1}H and ^{13}C-NMR chemical shift values were calculated according to GIAO (Gauge-Independent Atomic Orbital) method [26] and also TMS which an internal standard chemical shifts as solvent deuterated chloroform ($CDCI_3$). The frontier molecular orbital energy values, the highest occupied molecular orbital (HOMO) and the lowest unoccupied molecular orbital (LUMO), were calculated for the compounds. And some structure parameters were examined such as ionization potential, electron affinity electronegativity, chemical hardness-softness, etc.

Table 1. Crystallographic data and structure refinement parameters for the compounds.

	Compound I	**Compound II**
CCDC deposition no.	1560345	1560339
Color	Yellow	Yellow
Chemical formula	$C_{20}H_{20}O$	$C_{16}H_{17}ClO$
Formula weight	276.36	260.74
Temperature (K)	296	296
Wavelength (Å)	0.71073 Mo-Kα	0.71073 Mo-Kα
Crystal system	Monoclinic	Triclinic
Space group	$P2_1/n$	P-1
Unit cell parameters		
a, *b*, *c* (Å)	7.490 (8), 13.9353 (15), 15.0557 (14)	6.1638 (9), 9.4790 (15),12.764 (2)
α, β, γ (°)	94.681 (4)	88.812 (6), 84.727 (5), 73.132 (5)
Volume (Å^3)	1566.2 (17)	710.64 (19)
Z	4	2
D_{calc} (g/cm^3)	1.172	1.219
μ (mm^{-1})	0.07	0.26
F(000)	592	276
Crystal size (mm^3)	0.22 × 0.19 × 0.15	0.15 × 0.11 × 0.10
Diffractometer/measurement method	STOE IPDS 2/ω scan	STOE IPDS 2/ω scan
Index ranges	$-9 \le h \le 9$, $-17 \le k \le 17$, $-17 \le l \le 18$	$-8 \le h \le 8$, $-12 \le k \le 12$, $-17 \le l \le 17$
θ range for data collection (°)	$2.9 < \theta < 26$	$3.2 < \theta < 28.5$
Reflections collected	27081	29210
Independent/observed reflections	2953/2254	3566/2000
R_{int}	0.049	0.060
Refinement method	Full-matrix least-squares on F^2	Full-matrix least-squares on F^2
Goodness-of-fit on F^2	1.04	1.05
$\Delta\rho_{max}$, $\Delta\rho_{min}$ (e/Å^3)	0.23, −0.17	0.18, −0.21

According to Koopmans' Theory [27], ionization potential (*I*) and electron affinity (*A*) can be expressed as,

$$I=-E_{HOMO} \text{ and } A=-E_{LUMO} \quad (1)$$

electronegativity (χ) and chemical hardness (η) [28,29] can be calculated as,

$$\chi=(I+A)/2 \text{ and } \eta=(I-A)/2 \quad (2)$$

Similarly, other reactivity parameters are chemical softness (*S*) [30], electronic chemical potential (μ) [27b, 31] and electrophilicity index (ω) [32] which defined as,

$$S=1/2\eta,\ \mu=-(I+A)/2 \text{ and } \omega=\mu^2/2\,\eta, \quad (3)$$

respectively.

Also, NLO (Nonlinear Optical) behaviours of the structures were analysed and the total electric dipole moment μ_{tot} and its components $\mu_i(i\rightarrow x,y,z)$, the polarizability α_{ij}, the first-order hyperpolarizability β_{ijk} values and their components for the compounds were calculated with DFT/B3LYP/6-311G(d,p).

The total dipole moment μ_{tot} and the total polarizability α_{tot} values can be computable with the following equations [33];

$$\mu_{tot} = \left(\mu_x^2 + \mu_y^2 + \mu_z^2\right)^{1/2} \quad (4)$$

$$\alpha_{tot} = \left(\alpha_{xx} + \alpha_{yy+}\alpha_{zz}\right)/3 \quad (5)$$

The first-order hyperpolarizability is a third rank tensor and it has 27 components indicated as a 3 ×3 × 3 matrix but Klienman symmetry allows to reduce 10 components [34, 35] owing to $\beta_{xyy} = \beta_{yxy} = \beta_{yyx} = \cdots$ in a similar way, other components will also be equal to the same value. The magnitude value of the first-order hyperpolarizability using the remaining components, β_{xxx} , β_{xxy} , β_{xyy} , β_{yyy} , β_{xxz}, β_{xyz} , β_{yyz} , β_{xzz} , β_{yzz} , β_{zzz} , can be calculated with;

$$\beta_{tot} = \left[(\beta_{xxx} + \beta_{xyy} + \beta_{xzz})^2 + (\beta_{yyy} + \beta_{yzz} + \beta_{yxx})^2 + (\beta_{zzz} + \beta_{zxx} + \beta_{zyy})^2\right]^{1/2} \quad (6)$$

Polarizability's unit was converted into esu (electrostatic unit), (1 a.u=0.1482×10^{-24} esu) and first-order hyperpolarizability's unit was converted into esu, (1 a.u=8.6393×10^{-33} esu) [36].

4. Results and discussion

4.1. Reaction yields

The results obtained according to different methods applied in the synthesis process of the compounds are given in the Table 2. As can be seen in the Table 2, in general reaction times were decreased under

microwave. When the reactions were generated by sonication with temperature controlled, reaction yields have become more improvement than microwave and conventional methods.

Table 2. Effect of changes in methods on reaction yield.

Compounds	Microwave/Time(min): isolated yield (%)	Sonication/Time(min) : isolated yield (%)	Conventional/Time(min): isolated yield (%)
I	15 : 80	360:87	720:78
II	15 : 85	360:90	720:80

Table 3. Hydrogen bonding geometry for the compound I and II.

D—H…A	D—H (Å)	H···A (Å)	D···A (Å)	D—H···A (°)
Compound I				
C7—H7···O1^{i}	0.93	2.52	3.362(4)	150
Compound II				
C16—H17···O1^{ii}	0.93	2.50	3.220(3)	134

Symmetry code: (i) −*x*+3/2, *y*−1/2, −*z*+3/2, (ii) −*x*−2, −*y*+2, −*z*.

4.2. Description of the single-crystal structures

In this study, two crystal structures containing cyclohexenone were clarified by x-ray diffraction method. ORTEP drawings of the compounds are shown in Figure 2-(a) and (b). The compound **I** contains naphthalene group together with cyclohexenone. This structure is monoclinic having the space group $P2_1/n$, with four molecules per unit cell. Similarly, the compound **II** contains chlorophenyl ring together with cyclohexenone and this structure is triclinic having the space group P-1 with two molecules in unit cell. When we look at the literature, the polymorph of compound **II** appears in monoclinic form [37].

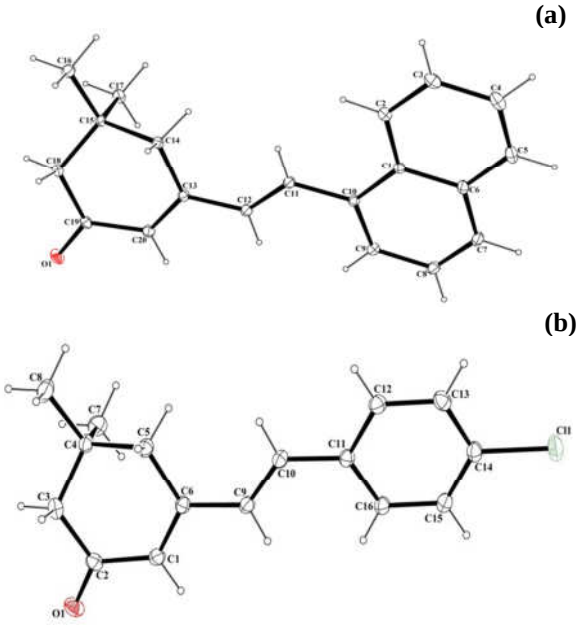

Figure 2. a) An ORTEP-3 view of the compound **I**, b) An ORTEP-3 view of the compound **II**.

In the compound **I**, $C_{20}H_{20}O$, dihedral angle between the 5,5-dimethylcyclohex-2- enone moiety and naphthalene group is 19.22°. The dimethylcyclohex ring (C19-C20) shows an envelope conformation. The C19-O1 bond length is a little shorter than literature values [38,39]. In the compound **I** structure, the C7—H7···O1 intermolecular interaction observed. In the compound **II,** $C_{16}H_{17}ClO$, dihedral angle between the 5,5-dimethylcyclohex-2-enone moiety and chlorophenyl group is 20.24°. The dimethylcyclohex ring (C1-C2) shows an envelope conformation. Similarly, C2-O1 bond length is a little shorter than literature values. In the compound **I** structure, the C16—H17···O1 intermolecular interaction observed. Details can be seen in Table 3.

4.3. Optimized structure analysis

Some of the selected structural parameters such as bond lengths and angles, torsion angles over the optimized geometries of the compounds were compared with the crystallographic values and the results were given in Table 4. As can be seen from the Table 4, carbon-oxygen double bond lengths are 1.233 Å as crystallographic, 1.219 Å as theoretical for the compound **I,** 1.222 Å crystallographic, 1.219 Å as theoretical for the compound **II.** These values are compatible with each other and as well as with typical C=O length of 1.22Å [40]. C=C double bond lengths, C13-C20, C11-C12, are 1.355, 1.349 Å theoretically for compound **I**, C1-C6, C9-C10, are 1.356, 1.348 Å theoretically for compound **II.** In a similar study, these lengths were indicated as 1.383, 1.385 Å for the DFT/6-311++G(d,p) [41]. For the compound **II**, C-Cl bond length is 1.740 Å as crystallographic value, 1.756 Å as theoretical value and in another study involving chlorophenyl group, this length was indicated as 1.755 Å for the DFT/6-31++G(d) [42]. Conjugated diene group bond angles, C11-C12-C13 for the compound **I**, are stated as 127.8, 126.2˚, C10-C9-C6 for the compound **II,** 126.8, 126.1˚ experimental and theoretical respectively.

Table 4. Some selected structure parameters of the compounds.

Parameters	Compound I		Parameters	Compound II	
	Exp.	DFT/B3LYP/ 6-311G(d,p)		Exp.	DFT/B3LYP/ 6-311G(d,p)
Bond Lengths (Å)					
C19-O1	1.233 (4)	1.219	C2-O1	1.222 (2)	1.219
C13-C20	1.344 (4)	1.355	C1-C6	1.346 (4)	1.356
C12-C13	1.455 (4)	1.454	C6-C9	1.456 (3)	1.454
C11-C12	1.321 (4)	1.349	C9-C10	1.326 (3)	1.348
C10-C11	1.476 (4)	1.466	C10-C11	1.467 (2)	1.462
C19-C20	1.457 (4)	1.468	C2-C1	1.453 (3)	1.468
C15-C16	1.522 (4)	1.537	C4-C7	1.530 (3)	1.541
C15-C17	1.526 (4)	1.541	C14-Cl1	1.740 (19)	1.756
C14-$H_{a,b}$	0.970	1.094-1.098	C5- $H_{a,b}$	0.970	1.094-1.098
C16-$H16_{a,b,c}$	0.960	1.094-1.093-1.094	C8-$H8_{a,b,c}$	0.960	1.094-1.093- 1.094
Bond Angles (°)					
O1-C19-C20	120.8 (3)	121.6	O1-C2-C1	121.8 (2)	121.5
O1-C19-C18	121.8 (3)	121.8	O1-C2-C3	121.6 (3)	121.9
C20-C13-C12	119.2 (3)	119.1	C1-C6-C9	119.8 (17)	119.0
C12-C11-C10	125.9 (3)	125.2	C9-C10-C11	126.8 (18)	127.0
C11-C12-C13	127.8 (3)	126.2	C10-C9-C6	126.8 (17)	126.1
C12-C13-C14	120.2 (2)	120.3	C9-C6-C5	119.6 (16)	120.3
C1-C10-C11	121.1 (2)	120.7	C10-C11-C12	120.0 (17)	118.8
C2-C1-C6	117.1 (3)	117.8	C12-C11-C16	117.7 (17)	117.5
C2-C1-C10	123.4 (3)	123.1	C8-C4-C5	109.4 (17)	109.1
C16-C15-C14	110.0 (2)	109.2	C13-C14-Cl1	119.7 (16)	119.6
C10-C11-H11	117.1	116.2	C15-C14-Cl1	119.0 (17)	119.4
C11-C12-H12	116.1	118.7	C10-C9-H9	116.6	119.3
Torsion Angles (°)					
O1-C19-C20-C13	-175.8 (3)	177.249	C6-C1-C2-O1	177.2 (19)	177.1
C15-C18-C19-O1	-156.5 (3)	-149.432	O1-C2-C3-C4	-149.0 (19)	-149.1
C10-C11-C12-C13	177.4 (3)	-178.676	C6-C1-C2-C3	-5.6 (3)	-4.7
C10-C1-C2-C3	179.6 (3)	-179.840	C6-C9-C10-C11	-178.38 (17)	179.1
C11-C12-C13-C14	2.5 (5)	1.491	C5-C6-C9-C10	2.1 (3)	1.4
C11-C12-C13-C20	-175.2 (3)	-177.040	C1-C6-C9-C10	-176.0 (19)	-177.1

In general, when these types of comparisons are made, it was observed that the geometric parameter values are compatible with each other. It is thought that the small differences are caused by the acceptance of the compounds in the solid phase at the crystallographic analysis process and in the gas phase at the theoretical analysis process.

4.4. Spectral analysis

4.4.1. Vibrational frequencies

The anharmonic and scaled harmonic vibrational frequencies of the compounds were recorded in the range of 4000-400 cm^{-1}. Theoretical frequencies have been compared with experimental spectral values and given in Table 5. The GaussView molecular visualization program [20] has been very helpful in interpreting the stretching and bending vibration assignments.

Compound **I** has 41 atoms, and 117 normal modes of vibrations which consist 40 stretching and 77 bending vibrations while compound **II** has 35 atoms, and 99 normal modes of vibrations which consist 34 stretching and 65 bending vibrations. Both compounds contain characteristic C-H, C=O, and C=C stretching vibration bands. Symmetric and asymmetric C-H stretching vibrations are observed at 3000 cm^{-1} and above for aromatic and diene groups, 3000-2900 cm^{-1} in region for cyclohexenone and methyl groups, as spectral and theoretical. These values are in agreement with the region of 3000-3100cm^{-1}, where characteristic C-H stretching bands observed especially in the aromatic groups [43-44]. The carbonyl group C=O bond stretching vibration modes are appeared at 1646 cm^{-1} as experimental, 1683 cm^{-1} as theoretical for compound **I**, 1655 cm^{-1} as experimental, 1685 cm^{-1} as theoretical for compound **II.** This vibration mode is one of the most characteristic bands on the whole IR spectrum and is observed in the ketone aldehyde groups in the interval of 1740-1725 cm^{-1} [45]. But, stretching frequencies of the compound **I** and **II** were recorded at lower values due to the effect of the conjugation. A similar mesomeric effect was also observed in another study [46] involving the cyclohexanone group and the same band was recorded as 1645 cm^{-1} spectral, 1666 cm^{-1} theoretical with DFT/B3LYP/6-31G(d) level. The C=C stretching absorption band is another major characteristic peak and generally appeared in the region 1625-1590 cm^{-1}[47] for conjugated alkene groups, this band is recorded at 1606 cm^{-1}, 1611 $cm^{-1}$for the compound **I**, 1616 cm^{-1}, 1614-1583 cm^{-1} for the compound **II,** as experimental and theoretical, respectively. Aromatic ring C=C stretching vibrational modes are observed as 1578 cm^{-1} spectral value, 1578-1497 cm^{-1} theoretical value for the compound **I**, 1579 cm^{-1} spectral value, 1549 cm^{-1}

theoretical value for compound **II**, and these wavenumbers values in good agreement with the literature [45,48-50]. C-H in plane and out-of plane bending vibrations bands belong to compounds were assigned at around range 1486-792 cm^{-1} experimentally, 1466-783 cm^{-1} theoretically.

4.4.2. ^{1}H and ^{13}C-NMR chemical shifts

Experimental and theoretical ^{1}H-NMR and ^{13}C-NMR chemical shifts values were recorded within the range of 8.15-1.16 ppm, 200.19-28.58 ppm for the compound **I**, 7.42-1.11 ppm, 200.06-28.48 ppm for the compound **II**. As calculated these values with GIAO method were obtained within the range of 8.41-0.79 ppm, 203.64-27.13 ppm for compound **I**, 8.05-0.73 ppm, 203.55-27.07 ppm for compound **II**. All experimental and theoretical chemical shift values of compounds are shown in Table 6.

Table 5. Comparison of the experimental and theoretical vibrational frequencies of the compounds.

Compound I			Compound II		
Assignment*	**Experimental (cm^{-1})**	**Calculated (cm^{-1})**	**Assignment***	**Experimental (cm^{-1})**	**Calculated (cm^{-1})**
ν_s(C-H)$_{naphthalene}$	3054	3097-3088	ν_s(C-H)$_{chlorophenyl}$	3035	3101
ν_{as}(C-H)$_{naphthalene}$	3027	3062-3059	ν_{as}(C-H)$_{chlorophenyl}$	3027	3067-3084
ν_s(C-H)$_{methyl}$	2964	2989	ν_s(C-H)$_{methyl}$	2951	2990
ν(C=O)	1646	1683	ν_s(C-H)$_{methylene}$	2880	2904
ν(C=C)$_{alkene}$	1606	1611	ν(C=O)	1655	1685
ν(C=C)$_{naphthalene}$	1578	1578-1497	ν(C=C)$_{alkene}$	1616	1614-1583
α(CH)$_{methyl}$	1455	1458	ν(C=C)$_{chlorophenyl}$	1579	1549
γ(CH)$_{methyl}$	1361	1358	α(CH)$_{methyl}$	1486	1466
γ(CH)$_{alkene}$	1301	1302	γ(CH)$_{methyl}$	1367	1359
γ(CH)$_{naphthalene}$	1247	1243	γ(CH)$_{alkene}$	1297	1294
δ(CH)$_{naphthalene}$	967	966	γ(CH)$_{chlorophenyl}$	1243	1280
ω(CH)$_{naphthalene}$	792	783	δ(CH)$_{chlorophenyl}$	968	942
$\beta_{naphtalene}$	768	778	$\theta_{chlorophenyl}$	836	840
$\theta_{cyclohexenone}$	-	653	$\theta_{cyclohexenone}$	828	826

**ν; stretching (s; symmetric, as; asymmetric), α; scissoring, γ; rocking, ω; wagging, δ; twisting, β; ring deformation, θ; ring breathing.*

Table 6. Experimental and theoretical ^{13}C-NMR and ^{1}H-NMR isotropic chemical shifts for the compounds.

Compound I			Compound II		
Atom	**Experimental (ppm)**	**Theoretical (ppm)**	**Atom**	**Experimental (ppm)**	**Theoretical (ppm)**
C1	131.24	138.06	C1	129.06	135.01
C2	123.30	129.19	C2	200.06	203.55
C3	126.52	132.90	C3	51.40	55.96
C4	126.07	132.33	C4	127.46	40.78
C5	128.83	135.47	C5	39.02	42.43
C6	131.63	140.11	C6	154.22	164.07
C7	129.40	136.73	C7	33.32	29.90
C8	125.63	131.78	C8	28.48	33.70
C9	124.30	131.24	C9	128.34	136.66
C10	133.72	141.86	C10	134.49	141.03
C11	133.39	141.16	C11	133.48	141.31
C12	132.37	140.12	C12	130.13	139.06
C13	154.69	164.49	C13	130.13	135.68
C14	51.47	42.50	C14	134.75	150.07
C15	39.25	40.97	C15	128.90	135.67
C16	33.40	33.98	C16	128.90	130.88
C17	28.58	27.13	H1	6.08	6.06
C18	123.20	124.44	H3$_{a,b}$	2.27	2.38-2.08
C19	200.19	203.64	H5$_{a,b}$	2.46	2.45-2.40
C20	127.36	134.62	H7$_{a,b,c}$	1.11	1.46-0.79-0.73
H2	8.15	8.41	H8$_{a,b,c}$	1.11	1.22-1.14-1.09
H3,H4	7.74	7.89	H9	6.91	7.31
H5,H7	7.86	8.20	H10	6.91	7.04
H8	7.63-7.44	7.80	H12	7.34	7.38
H9	7.78	8.09	H13	7.34	7.46
H11,H12	6.97	7.29,7.27	H15	7.42	7.50
H14$_{a,b}$	2.35	2.64-2.63	H16	7.42	8.05
H16$_{a,b,c}$	1.16	1.29-1.17-1.17			
H17$_{a,b,c}$	1.16	1.55-0.88-0.79			
H18$_{a,b,c}$	2.59	2.43-2.10			
H20	6.13	6.13			

ppm; parts per million and for the numbering of the atoms is basis on Figure 2.

Carbonyl group carbons, C19 for compound **I** and C2 for compound **II**, have the highest chemical shift values, because the oxygen atom with electronegative character reduces the electron density around the carbons. The chemical shift value of C19 is observed at 200.19 ppm, 203.64, C2 is observed at 200.06 ppm, 203.55 ppm, as spectral and theoretical, respectively. These values are in agreement with the range of 150-220 ppm where the chemical shift values of carbonyl groups [51]. Alkene group, sp^2 hybridized C13 (with values 154.69/164,49 ppm-exp/theo) of the compound **I** and C6 (with values 154.69/164,49 ppm-exp/theo) of the compound **II** atoms have other high chemical shift values. Aromatic ring carbon atoms have given as expected the signal at 100-150 ppm [52,53], and C1 to C10 atoms, belonging naphthalene group for the compound **I**, are observed at 133.72-123.30 ppm experimentally, 141.86-129.19 ppm theoretically. The chemical shift values of C11 to C16 atoms, belonging chlorophenyl group for the compound **II**, are observed at 134.75-128.90 ppm experimentally, 150.07-130.88 ppm theoretically. The C14 atom has a higher chemical shift than the other carbon atoms; because of the chlorine atom with the electron withdrawing character has caused its resonance value to observe at downfield. A similar substitution effect depending on the ortho-para position has identified in the studies involving other chlorophenyl groups [54,55].

Aromatic protons chemical shift values are 8.15-7.78 ppm as spectral values, 8.41-7.80 ppm as computed values GIAO method for the compound **I**, 7.42-7.34 ppm as spectral values, 8.05-7.04 ppm as computed values GIAO method for the compound **II**. These values are compliance with each other and literature [56] that indicates as 6.0-8.5 ppm for aromatic protons. Alkene protons come to resonate in downfield with a secondary magnetic field effect due to the circulation of the double bound electrons in the magnetic field and are observed in the average range of 6.5-5 ppm [56]. In the present study, especially chemical shift values carbonyl group α-protons H20 and H1 have recorded 6.13 ppm as experimental and theoretical for the compound **I**, 6.08 ppm as experimental, 6.06 ppm as theoretical for the compound **II**. The methylene and methyl group protons have given low chemical shift values in upfield and assigned at average in the range of 2.3-0.7 ppm experimentally and theoretically. This range confirms that the protons attached to sp^3 hybridized carbon can be observed at 0-2 ppm [47].

4.5. Some chemical reactivity parameters

The HOMO and LUMO energy values for the compound **I** and **II** are examined with DFT/B3LYP/6-311G(d,p) level in gas phase to have information about the chemical stability of compounds. The HOMO-LUMO energies are associated with the ability of electron donate and acceptor of molecules. And the energy gap between $\Delta E=E_{HOMO}-E_{LUMO}$ value gives information about kinetic stability, polarizability and chemical hardness and softness of the molecules [57]. A large energy gap value indicates high kinetic stability, low chemical reactivity [58]. The energy gap value is, ΔE=3.59 eV for the compound **I**, 3.80 ev for the compound **II**. According to these values, it can be said that compound **I** has softer, a lower kinetic stability and a higher chemical reactivity than compound **II**.

Table 7. Some chemical reactivity features of the compounds.

	Compound I	***Compound II***
$\mathbf{E_{TOTAL}}$ (*Hartree*)	-849.60933515	-1155.55827396
$\mathbf{E_{HOMO}}$ *(eV)*	-5.9552	-6.2940
$\mathbf{E_{LUMO}}$ *(eV)*	-2.3627	-2.4931
I *(eV)*	5.9552	6.2940
A *(eV)*	2.3627	2.4931
$\boldsymbol{\chi}$ *(eV)*	4.1590	4.3935
$\boldsymbol{\eta}$ *(eV)*	1.7962	1.9004
S *(eV^{-1})*	0.2783	0.2630
$\boldsymbol{\mu}$ *(eV)*	-4.1590	-4.3935
$\boldsymbol{\omega}$ *(eV)*	4.8149	5.0786

Table 8. The electric dipole moment, polarizability and first hyperpolarizability of the compounds.

	Compound I	**Compound II**
	B3LYP/6-311G(d,p)	B3LYP/6-311G(d,p)
Electric Dipole Moment (D)		
μ_x	-3.7525	1.1525
μ_y	2.5967	-3.3411
μ_z	1.1855	-0.3194
$\boldsymbol{\mu_{tot}}$	4.7148	3.5487
Polarizability ($x10^{-24}$esu)		
α_{xx}	59.7320	57.8562
α_{xy}	-3.8094	-4.6165
α_{yy}	35.9418	27.7195
α_{xz}	-2.4538	0.5255
α_{yz}	-2.1724	1.2394
α_{zz}	19.2865	15.6977
$\boldsymbol{\alpha_{tot}}$	38.3201	33.7578
First Hyperpolarizability ($x10^{-33}$esu)		
β_{xxx}	29266.2302	-32549.63
β_{xxy}	964.4063	1588.451
β_{xyy}	-891.9190	691.0706
β_{yyy}	121.6856	-924.8111
β_{xxz}	-1662.1060	-515.558
β_{xyz}	37.2578	219.4166
β_{yyz}	-24.0059	185.1557
β_{xzz}	215.0873	-418.5473
β_{yzz}	590.6659	-445.1883
β_{zzz}	179.6505	-514.6439
$\boldsymbol{\beta_{tot}}$	28678.1200	32288.9099

As it is known ionization potential (*I*) is the minimum energy required to remove an electron from an atom or molecule, electron affinity (*A*) is

described as the change in energy when an electron is added to a neutral atom in the gas phase, chemical hardness and softness are defined as a measure of inhibition of intramolecular charge transfer [59]. Some reactivity parameters defined by the equations (1), (2) and (3) are given in Table 7.

In general, it can be said that compound **II** has higher reactivity parameters than compound **I**. When the ionization potentials are examined, it can be said that compound **I** has better electron donating properties than compound **II**, while electron affinity values are examined compound **II** has better electron accepting properties than compound **I**. The compound **II** has the higher chemical hardness (η), the lower chemical softness (S) than compound **I**, so intramolecular charge transfer may be less possible. Also, these results support the view that we have already mentioned about with respect to the fact that compound **II** has a higher ΔE value than **I**. A good electrophile has a high chemical potential and low chemical hardness value [60], in which case compound **I** exhibit better electrophile character than compound **II**.

4.6. NLO properties

The design of materials with NLO character is one of the current research topics and they have been used optical modulation, optical switching, optical logic, optical memory for the emerging technologies in the area of telecommunications, transmission of optical signals, optical interconnection, sensing, frequency shifting, signal processing, laser and in the other application of optoelectronics [61-65].

In order to be able to examine the NLO behaviour of the compound **I** and **II**, the values of the total electric dipole moment, μ_{tot}, the polarizability, α_{ij}, the first-order hyperpolarizability, β_{ijk}, values and their components have been calculated with equations (4), (5) and (6). The results obtained are given in Table 8. The calculated total dipole moment, μ_{tot}, total polarizability, α_{tot}, first-order hyperpolarizability, β_{tot}, values are 4.7148 D, 38.3201x10^{-24} esu, 28678.1200 x10^{-33} esu for the compound **I**, 3.5487 D, 33.7578 x10^{-24} esu, 32288.9099 x10^{-33} esu for the compound **II**, respectively.

The same parameters have been calculated for the urea molecule used as the threshold value in NLO applications. μ_{tot}, α_{tot}, and, β_{tot}, values of the urea are calculated 3.6209 D, 4.1499 x10^{-24} esu, 603.1465 x10^{-33} esu. The μ_{tot} value of the compound **I** has found higher, while the compound **II** has found slightly smaller than the value of the urea molecule. α_{tot} and β_{tot} values of the compound **I** are 9.23 and 47.5 times, of the compound **II** are 8.13 and 53.5 greater from the value of urea. As a result of these comparisons compound **II**, which is chlorophenyl derivative of isophorone, exhibits a higher NLO behaviour than compound **I** or naphthyl derivative.

4.7. Antioxidant activity

Antioxidant activity of the compounds various fraction (10-100 µg/mL) was determined using three different assays. Antioxidant assay of extracts for the compounds are shown in Figure 3.

DPPH Free Radical Scavenging Activity

It was found to be used in -vitro antioxidant activity depend on 1,1-diphenyl-2-picryl-hydrazyl (DPPH·) compound. The violet colored were disappeared when reaction started with compounds and standards as BHA, BHT, α-tocopherol free radical scavenging activity was calculated Brand-Williams methods [66]. The percent inhibition activity was calculated using the following equation:

Free radical scavenging effect %= $[(A_0\text{-}A_s)/A_0].100$

(A_0= the control absorbance and A_s= the sample solution absorbance)

Reducing Activity

The reducing activity is known the important detail of antioxidation according to Oyaizu method [67]. In this method, we used potassium ferricyanide [$K_3Fe(CN)_6$], TCA, FeCl3, and absorbance was measured 700 nm in the microplate reader. The compounds showed rises of activity depend on concentration.

Metal Chelating Activity

Measurements of metal chelating activity of compounds were estimated according to the method of Decker and Welch [68]. The chelating activity of the sample on Fe^{2+} was compared with that of EDTA at the same concentrations and was measured at 562 nm.

Metal chelating activity (%) = $[(A_0\text{-}A_1)/A_0].100$

5. Conclusion

In this paper, *(E)-5,5-dimethyl-3-(2-(naphyhalen-1-yl)vinyl)-cyclohex-2-enone* and *(E)-3-(4-chlorostyryl)-5,5-dimethylcyclohex-2-enone* compounds were synthesized with conventional thermal, microwave and sonication methods. It was determined that the microwave method according to the reaction times, and the temperature controlled sonication method according to the yield values are more advantageous than the others.

Compound **I** and **II** were characterized by spectral methods (X-ray crystallographic technique, FT-IR, ^{1}H-NMR, and ^{13}C-NMR) and the results obtained

were compared with those obtained from quantum mechanical methods (DFT/B3LYP/6-311G(d,p)).

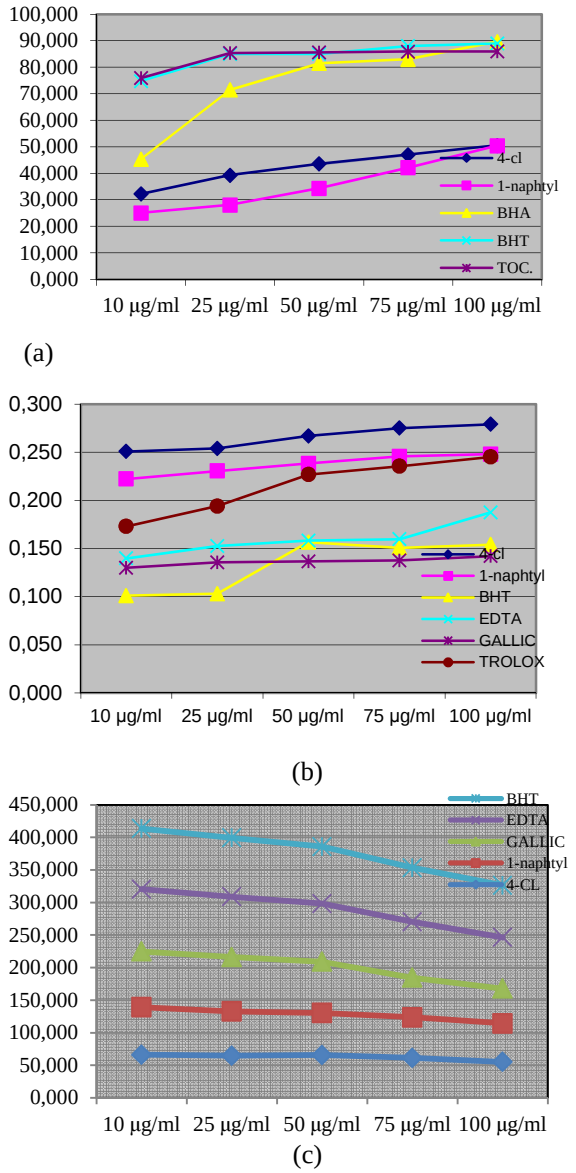

Figure 3. Antioxidant assay of extracts for the compounds. ((a) *DPPH Radical scavenging*, (b) *Reduction Activity*, (c) *Metal Chelating Activity*)

It can be said that the spectrally recorded and calculated parameters of the compounds are generally compatible with each other and with similar studies. In comparison experimental with theoretical values, it is seen that most of the parameters are slightly different, as experimental results over the solid state, theoretical ones over the gas phase. Some chemical reactivity parameters of the compounds were examined and it can be said that compound **II** has a better electron acceptor character, more electronegative and harder molecule structure than compound **I**. Nonlinear optical behaviours of the compounds were investigated and the chlorophenyl derivative of isophorone (**II**) was found to be a better NLO material candidate than the naphthyl derivative (**I**). Also, antioxidant activity properties of the compound determined using three different assays. When the results of these analyses are examined, it has been observed that compound **I** exhibits higher DPPH free radical scavenging and reducing activity, and compound **II** exhibits higher metal chelating activity. We hope that the results of this study will provide useful information for other isophorone derivatives.

Acknowledgments

We gratefully acknowledge the financial support of this work by the Amasya University Scientific Research Foundation (FMB-BAP 16-0216). All samples have been identified in the AUMAULAB Central Laboratory in Amasya University, Turkey. The authors acknowledge Scientific and Technological Research Application and Research Center, Sinop University, Turkey, for the use of the Bruker D8 QUEST diffractometer.

Appendix A. Supplementary Materials

The FT-IR, ^{1}H and ^{13}C-NMR spectrums of the compounds are given in the Supplementary Materials.

References

[1] Agency for toxic substances and disease registry (ATSDR), Toxicological profile for isophorone, Department of Health and Human Services, Public Health Service, Atlanta, GA, U.S., (1989).

[2] Kataoka, H., Terada, Y., Inoue, Y. and Mitani, K., Determination of isophorone in food samples by solid-phase microextraction coupled with gas chromatography-mass spectrometry, **Journal of Chromatography A,** 1155, 1, 100-104, (2007).

[3] Environmental health criteria 174:Isophorone, World Health Organization for the International Programme on Chemical Safety, Geneva, WHO, (1995).

[4] Samimi, B., Exposure to isophorone and other organic solvents in a screen printing plant, **The American Industrial Hygiene Association Journal**, 43, 1, 43-48, (1982).

[5] Shackelford, W.M. and Keith, L.H., Frequency of organic compounds identified in water, Environmental Research Laboratory, Office of Research and Development, U.S.

Environmental Protection Agency, Athens, Ga., (1976).

[6] Horng, J.Y. and Huang, S.D., Determination of the semi-volatile compounds nitrobenzene, isophorone, 2, 4-dinitrotoluene and 2, 6-dinitrotoluene in water using solid-phase microextraction with a polydimethylsiloxane-coated fibre, **Journal of Chromatography A**, 678, 2, 313-318, (1994).

[7] Sasaki, K., Tagata, H., Kawakami, H., Nagasaki, T., Nemoto, S. and Maitani, T., Determination of isophorone in foods, **Journal of the Food Hygienic Society of Japan**, 46, 1, 28-32, (2005).

[8] Camarasa, J.G. and Serra-Baldrich, E., Allergic dermatitis caused by gold. Description of a new case, **Medicina Cutanea Ibero-Latino-Americana**, 17, 3, 187-188, (1989).

[9] Rademaker, M., Occupational epoxy resin allergic contact dermatitis, **Australasian Journal of Dermatology**, 41, 4, 222-224, (2000).

[10] Clarke, C. W. and Aldons, P. M., Isophorone diisocyanate induced respiratory disease (IPDI), **Australian and New Zealand Journal of Medicine**, 11, 3, 290-292, (1981).

[11] Bucher, J.R., Huff, J. and Kluwe, W. M., Toxicology and carcinogenesis studies of isophorone in F344 rats and B6C3F1 mice, **Toxicology**, 39, 2, 207-219, (1986).

[12] Yamada, Y., Yoshikawa, N., Sasai, H. and Shibasaki, M., Direct catalytic asymmetric aldol reactions of aldehydes with unmodified ketones, **Angewandte Chemie International Edition**, 36, 17, 1871-1873, (1997).

[13] Kergomard, A., Renard, M.F. and Veschambre, H., Microbiological reduction of alpha, beta-unsaturated ketones by Beauveria sulfurescens, **The Journal of Organic Chemistry**, 47, 5, 792-798, (1982).

[14] Conti, M., Cyclopentenone: a special moiety for anticancer drug design, **Anti-cancer Drugs**, 17, 9, 1017-1022, (2006).

[15] Stoe & Cie, X-AREA (Version 1.18), Stoe & Cie GmbH, Darmstadt, Germany, (2002).

[16] Sheldrick, G.M., SHELXS-97, Program for the Solution of Crystal Structures, University of Gottingen, (1997).

[17] Sheldrick, G.M., SHELXL-2014/7: Program for the Solution of Crystal Structures, University of Göttingen, Göttingen, Germany, (2014).

[18] Farrugia, L.J., WinGX suite for small-molecule single-crystal crystallography, **Journal of Applied Crystallography**, 32, 4, 837-838, (1999).

[19] Frisch, M.J., Trucks, G.W., Schlegel, H.B., Scuseria, G.E., Robb, M.A., Cheeseman, J.R., Scalmani, G., Barone, V., Mennucci, B., Petersson, G.A., Nakatsuji, H., Caricato, M., Li, X., Hratchian, H.P., Izmaylov, A.F., Bloino, J., Zheng, G., Sonnenberg, J.L., Hada, M., Ehara, M., Toyota, K., Fukuda, R., Hasegawa, J., Ishida, M., Nakajima, T., Honda, Y., Kitao, O., Nakai, H., Vreven, T., Montgomery, Jr., J.A., Peralta, J. E., Ogliaro, F., Bearpark, M., Heyd, J.J., Brothers, E., Kudin, K.N., Staroverov, V.N., Kobayashi, R., Normand, J., Raghavachari, K., Rendell, A., Burant, J.C., Iyengar, S.S., Tomasi, J., Cossi, M., Rega, N., Millam, J.M., Klene, M., Knox, J.E., Cross, J.B., Bakken, V., Adamo, C., Jaramillo, J., Gomperts, R., Stratmann, R.E., Yazyev, O., Austin, A.J., Cammi, R., Pomelli, C., Ochterski, J.W., Martin, R.L., Morokuma, K., Zakrzewski, V.G., Voth, G.A., Salvador, P., Dannenberg, J.J., Dapprich, S., Daniels, A.D., Farkas, Ö., Foresman, J.B., Ortiz, J.V., Cioslowski, J. and Fox, D.J., Gaussian 09, Revision E.01, Gaussian, Inc., Wallingford CT, (2009).

[20] Dennington, R., Keith, T. and Millam, J., GaussView, Version 5, Semichem Inc., Shawnee Mission, KS, (2009).

[21] a) Becke, A.D., Density-functional exchange-energy approximation with correct asymptotic behaviour, **Physical Review A**, 38, 6, 3098-3100, (1988). b) Becke, A.D., Density-functional thermochemistry. I, The effect of the exchange-only gradient correction, **The Journal of Chemical Physics**, 96, 3, 2155-2160, (1992).

[22] Ditchfield, R., Hehre, W.J. and Pople, J.A, Self-consistent molecular-orbital methods. IX. An extended Gaussian-type basis for molecular-orbital studies of organic molecules, **The Journal of Chemical Physics**, 54, 2, 724-728, (1971).

[23] Lee, C., Yang, W. and Parr, R.G., Development of the Colle-Salvetti correlation-energy formula into a functional of the electron density, **Physical Review B**, 37, 2, 785-789, (1988).

[24] Kowalczyk, I., Bartoszak-Adamska, E., Jaskólski, M., Dega-Szafran, Z. and Szafran, M, Structure of 1H-2-oxo-2, 3-dihydroimidazo [1,2-a] pyridinium perchlorate studied by X-ray diffraction, DFT calculations and by FTIR and NMR spectroscopy, **Journal of Molecular Structure**, 976, 1, 119-128, (2010).

[25] Merrick, J.P., Moran, D. and Radom, L., An evaluation of harmonic vibrational frequency scale factors, **The Journal of Physical Chemistry A**, 111, 45, 11683-11700, (2007).

[26] Cheeseman, J.R., Trucks, G.W., Keith, T.A. and Frisch, M.J., A comparison of models for calculating nuclear magnetic resonance shielding tensors, **The Journal of Chemical Physics**, 104, 14, 5497-5509, (1996).

[27] a) Koopmans, T., Ordering of wave functions and eigenenergies to the individual electrons of an atom, **Physica**, 1, 1, 104-113, (1933). b) Vektariene, A., Vektaris, G. and Svoboda, J., A theoretical approach to the nucleophilic behavior of benzofused thieno [3,2-b] furans using DFT and HF based reactivity descriptors, **Arkivoc: Online Journal of Organic Chemistry**, vii, 311-329 (2009).

[28] Mulliken, R. S., A new electroaffinity scale; together with data on valence states and on valence ionization potentials and electron affinities, **The Journal of Chemical Physics**, 2, 11, 782-793, (1934).

[29] a) Pearson, R.G., Hard and soft acids and bases, **Journal of the American Chemical Society**, 85, 22, 3533-3539, (1963). b) Pearson, R.G., Hard and soft acids and bases, HSAB, part 1: Fundamental principles, **Journal of Chemical Education**, 45, 9, 581-587, (1968). c) Pearson, R.G., Maximum chemical and physical hardness, **Journal of Chemical Education,** 76, 2, 267-270, (1999).

[30] Pearson, R.G., Absolute electronegativity and hardness correlated with molecular orbital theory, **Proceedings of the National Academy of Sciences**, 83, 22, 8440-8441, (1986).

[31] Parr, R.G. and Pearson, R.G., Absolute hardness: companion parameter to absolute electronegativity, **Journal of the American Chemical Society**, 105, 26, 7512-7516, (1983).

[32] Chattaraj, P.K. and Roy, D.R., Update 1 of: Electrophilicity index, **Chemical Reviews**, 107, 9, PR46–PR74, (2007).

[33] Hernández-Paredes, J., Glossman-Mitnik, D., Duarte-Moller, A. and Flores-Holguín, N., Theoretical calculations of molecular dipole moment, polarizability, and first hyperpolarizability of glycine–sodium nitrate, **Journal of Molecular Structure: THEOCHEM**, 905, 1, 76-80, (2009).

[34] Prashanth, J., Ramesh, G., Naik, J.L., Ojha, J.K., Reddy, B.V. and Rao, G.R., Molecular structure, vibrational analysis and first order hyperpolarizability of 4-methyl-3-nitrobenzoic acid using density functional theory, **Optics and Photonics Journal**, 5, 91-107, (2015).

[35] a) Kleinman, D.A., Nonlinear dielectric polarization in optical media, **Physical Review**, 126, 6, 1977-1979, (1962). b) Ramalingam, S., Karabacak, M., Periandy, S., Puviarasan, N. and Tanuja, D., Spectroscopic (infrared, Raman, UV and NMR) analysis, Gaussian hybrid computational investigation (MEP maps/HOMO and LUMO) on cyclohexanone oxime, **Spectrochimica Acta Part A: Molecular and Biomolecular Spectroscopy**, 96, 207-220, (2012).

[36] Suresh, S., Gunasekaran, S. and Srinivasan, S., Spectroscopic (FT-IR, FT-Raman, NMR and UV–Visible) and quantum chemical studies of molecular geometry, Frontier molecular orbital, NLO, NBO and thermodynamic properties of salicylic acid, **Spectrochimica Acta Part A: Molecular and Biomolecular Spectroscopy**, 132, 130-141, (2014).

[37] Fatima, Z., Senthilkumar, G., Vadivel, A., Manikandan, H. and Velmurugan, D, 3-[(E)-2-(4-Chlorophenyl)ethenyl]-5,5-dimethylcyclohex-2-en-1-one, **Acta Crystallographica Section E: Structure Reports Online**, 69, 7, o1121-o1121, (2013).

[38] Cha, J.H., Lee, J.K., Min, S.J., Cho, Y.S. and Park, J., (E)-2,2′-[3-(4-Chlorophenyl) prop-2-ene-1,1-diyl]bis(3-hydroxy-5,5-dimethylcyclohex-2-en-1-one), **Acta Crystallographica Section E: Structure Reports Online**, 69, 8, o1347-o1347, (2013).

[39] Boulebd, H., Bouraiou, A., Bouacida, S., Merazig, H. and Belfaitah, A., 3-Anilino-5, 5-dimethylcyclohex-2-enone, **Acta Crystallographica Section E: Structure Reports Online**, 70, 3, o233-o234, (2014).

[40] Allinger, N.L., Hirsch, J.A., Miller, M.A. and Tyminski, I.J., Conformational analysis, LXV, calculation by the Westheimer method of the structures and energies of a variety of organic molecules containing nitrogen, oxygen, and halogen, **Journal of the American Chemical Society**, 91, 2, 337-343, (1969).

[41] Koleva, B.B. and Kolev, T., Monoclinic and triclinic polymorphs of 2-{5, 5-dimethyl-3-[2-(2, 4, 6-trimethoxyphenyl) vinyl] cyclohex-2-enylidene} malononitrile—Solid-state linear-polarized IR-spectroscopy, DFT calculations and vibrational analysis, **Spectrochimica Acta Part A: Molecular and Biomolecular Spectroscopy**, 71, 3, 786-793, (2008).

[42] Parveen, S., Al-Alshaikh, M.A., Panicker, C.Y., El-Emam, A.A., Salian, V.V., Narayana, B. and Van Alsenoy, C., Spectroscopic investigations and molecular docking study of (2E)-1-(4-chlorophenyl)-3-[4-(propan-2-yl) phenyl] prop-2-en-1-one using quantum chemical calculations, **Journal of Molecular Structure**, 1120, 317-326, (2016).

[43] Silverstein, R.M., Webster, F.X., Kiemle, D.J. and Bryce, D.L, **Spectrometric identification of organic compounds**, 87, John Wiley & Sons, Hoboken, NJ, (2014).

[44] Raj, P.S., Shoba, D., Ramalingam, S. and Periandy, S., Spectroscopic (FT-IR/FT-Raman) and computational (HF/DFT) investigation and HOMO/LUMO/MEP analysis on 1, 1-difluoro-2-vinyl-cyclopropane, **Spectrochimica Acta Part A: Molecular and Biomolecular Spectroscopy**, 147, 293-302, (2015).

[45] Coates, J., **Interpretation of infrared spectra, a practical approach**, in Meyers, R. A., (Ed), *Encyclopedia of Analytical Chemistry*, John

Wiley & Sons Ltd, Chichester, 10815-10837, (2000).

[46] James, C., Raj, A.A., Reghunathan, R., Jayakumar, V.S. and Joe, I.H., Structural conformation and vibrational spectroscopic studies of 2, 6-bis (p-N, N-dimethyl benzylidene) cyclohexanone using density functional theory, **Journal of Raman Spectroscopy**, 37, 12, 1381-1392, (2006).

[47] Erdik, E., **Organik kimyada spektroskopik yöntemler**, Gazi Büro Kitabevi, Ankara, 111, (2008).

[48] Sathiyanarayanan, D.N., **Vibrational spectroscopy theory and application**, New Age International Publishers, New Delhi, 424, (2004).

[49] Krishnakumar, V., Manohar, S. and Nagalakshmi, R., Crystal growth and characterization of N-hydroxyphthalimide ($C_8H_5NO_3$) crystal, **Spectrochimica Acta Part A: Molecular and Biomolecular Spectroscopy**, 71, 1, 110-115, (2008).

[50] Singh, N.P. and Yadav, R.A., Optics spectroscopy-vibrational studies of trifluoromethyl benzene derivatives I: 2-amino, 5-chloro and 2-amino, 5-bromo benzotrifluorides, **Indian Journal of Physics**, 75, 4, 347-356, (2001).

[51] Brouwer, H. and Stothers, J.B., ^{13}C-Nuclear magnetic resonance studies. XVI.,^{13}C Spectra of some substituted acrylic acids and their methyl esters, A correlation of olefinic shieldings in α, β-unsaturated carbonyl systems, **Canadian Journal of Chemistry**, 50, 5, 601-611, (1972).

[52] Francioso, O., Sanchez-Cortes, S., Tugnoli, V., Ciavatta, C., Sitti, L. and Gessa, C., Infrared, raman, and nuclear magnetic resonance (^{1}H, ^{13}C, and ^{31}P) spectroscopy in the study of fractions of peat humic acids, **Applied Spectroscopy**, 50, 9, 1165-1174, (1996).

[53] Jacobsen, N.E., **NMR spectroscopy explained: simplified theory, applications and examples for organic chemistry and structural biology**, 29, John Wiley & Sons, Hoboken, NJ, (2007).

[54] Eryılmaz, S., Gül, M., İnkaya, E., İdil, Ö. and Özdemir, N., Synthesis, crystal structure analysis, spectral characterization, quantum chemical calculations, antioxidant and antimicrobial activity of 3-(4-chlorophenyl)-3a,4,7,7a-tetrahydro-4,7-methanobenzo[d] isoxazole, **Journal of Molecular Structure**, 1122, 219-233, (2016).

[55] Verma, A.K., Bishnoi, A. and Fatma, S., Synthesis, spectral analysis and quantum chemical studies on molecular geometry of (2E, 6E)-2, 6-bis (2-chlorobenzylidene) cyclohexanone: experimental and theoretical approaches, **Journal of Molecular Structure**, 1116, 9-21, (2016).

[56] Balcı, M., **Nükleer manyetik rezonans spektroskopisi**, 36, ODTÜ Yayıncılık, Ankara, (2004).

[57] Maache, S., Bendjeddou, A., Abbaz, T., Gouasmia, A. and Villemin, D., Molecular structure, hyperpolarizability, NBO and Fukui function analysis of a serie of 1, 4, 3, 5-oxathiadiazepane-4, 4-dioxides derived of proline, **Der Pharmacia Lettre**, 8, 11, 27-37, (2016).

[58] Aihara, J.I., Reduced HOMO− LUMO gap as an index of kinetic stability for polycyclic aromatic hydrocarbons, **The Journal of Physical Chemistry A**, 103, 37, 7487-7495, (1999).

[59] Günay, N., Pir, H. and Atalay, Y., L-Asparaginyum pikrat molekülünün spektroskopik özelliklerinin teorik olarak incelenmesi, **Sakarya Üniversitesi Fen Edebiyat Dergisi**, 1, 15-32, (2011).

[60] Eşme A. and Güneşdoğdu Sağdınç, S., Bazı Sudan Boyalarının Lineer, Lineer Olmayan Optik Özellikleri ve Kuantum Kimyasal Parametreleri, **Balıkesir Üniversitesi Fen Bilimleri Enstitüsü Dergisi**, 16, 1, 47-75, (2014).

[61] Nakano, M., Fujita, H., Takahata, M. and Yamaguchi, K., Theoretical study on second hyperpolarizabilities of phenylacetylene dendrimer: toward an understanding of structure− property relation in nlo responses of fractal antenna dendrimers, **Journal of the American Chemical Society**, 124, 32, 9648-9655, (2002).

[62] Prashanth, J., Ramesh, G., Naik, J.L., Ojha, J.K., Reddy, B.V. and Rao, G.R., Molecular structure, vibrational analysis and first order hyperpolarizability of 4-methyl-3-nitrobenzoic acid using density functional theory, **Optics and Photonics Journal**, 5, 3, 91-107, (2015).

[63] Sajan, D., Joe, H., Jayakumar, V.S. and Zaleski, J. Structural and electronic contributions to hyperpolarizability in methyl p-hydroxy benzoate, **Journal of Molecular Structure**, 785, 1, 43-53, (2006).

[64] Muthu, S. and Maheswari, J.U., Quantum mechanical study and spectroscopic (FT-IR, FT-Raman, ^{13}C, ^{1}H, UV) study, first order hyperpolarizability, NBO analysis, HOMO and LUMO analysis of 4-[(4-aminobenzene) sulfonyl] aniline by ab initio HF and density functional method, **Spectrochimica Acta Part A: Molecular and Biomolecular Spectroscopy**, 92, 154-163, (2012).

[65] Geskin, V.M., Lambert, C. and Brédas, J.L., Origin of high second-and third-order nonlinear optical response in ammonio/borato diphenylpolyene zwitterions: the remarkable

role of polarized aromatic groups, **Journal of the American Chemical Society**, 125, 50, 15651-15658, (2003).

[66] Brand-Williams, W., Cuvelier, M.E. and Berset, C., Use of a free radical method to evaluate antioxidant activity, **LWT-Food science and Technology**, 28, 1, 25-30, (1995).

[67] Oyaizu, M., Studies on products of browning reaction, **The Japanese Journal of Nutrition and Dietetics**, 44, 6, 307-315, (1986).

[68] Decker, E.A. and Welch, B., Role of ferritin as a lipid oxidation catalyst in muscle food, **Journal of Agricultural and Food Chemistry**, 38, 3, 674-677, (1990).

Appendix A. Supplementary Materials

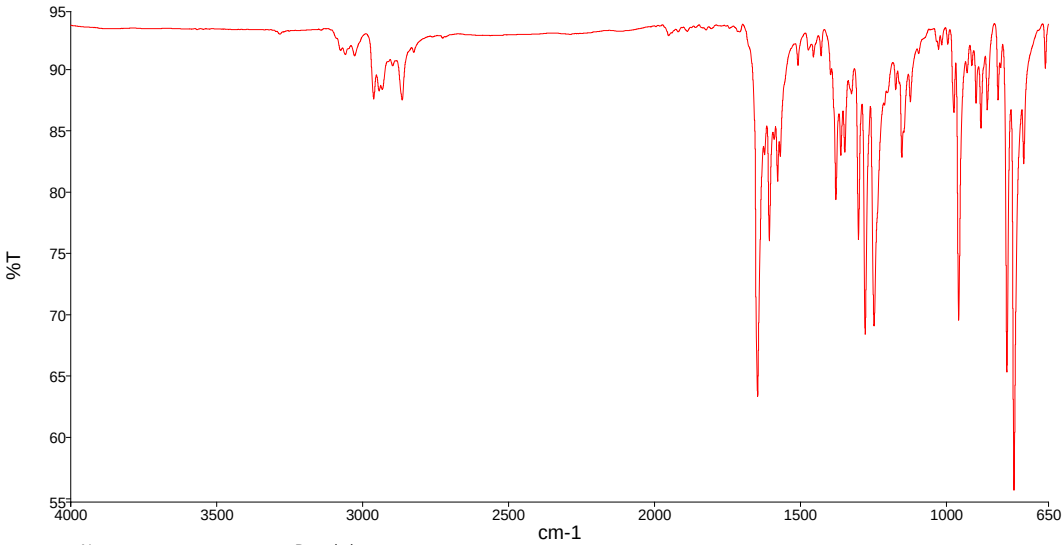

Figure S.1 The FT-IR spectrum of the compound I

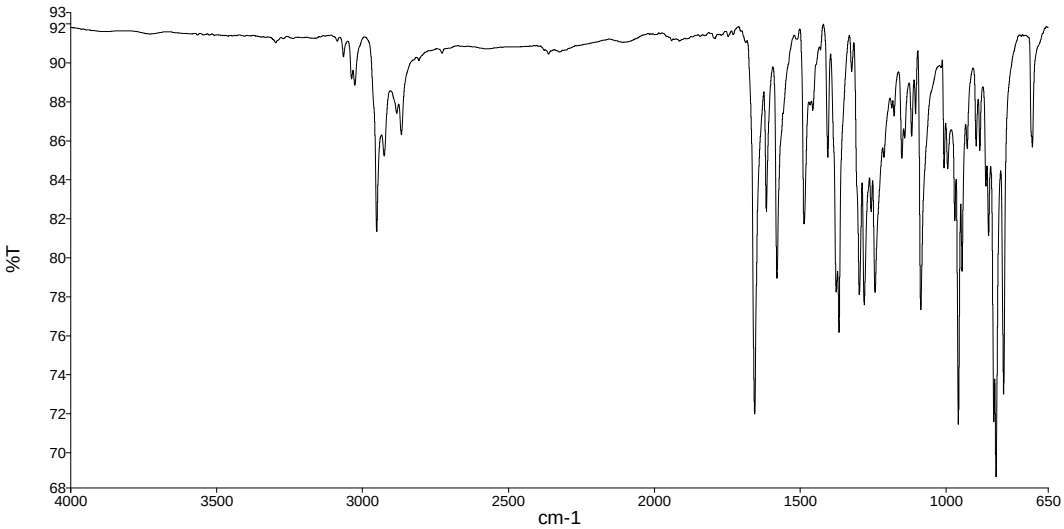

Figure S.2 The FT-IR spectrum of the compound II

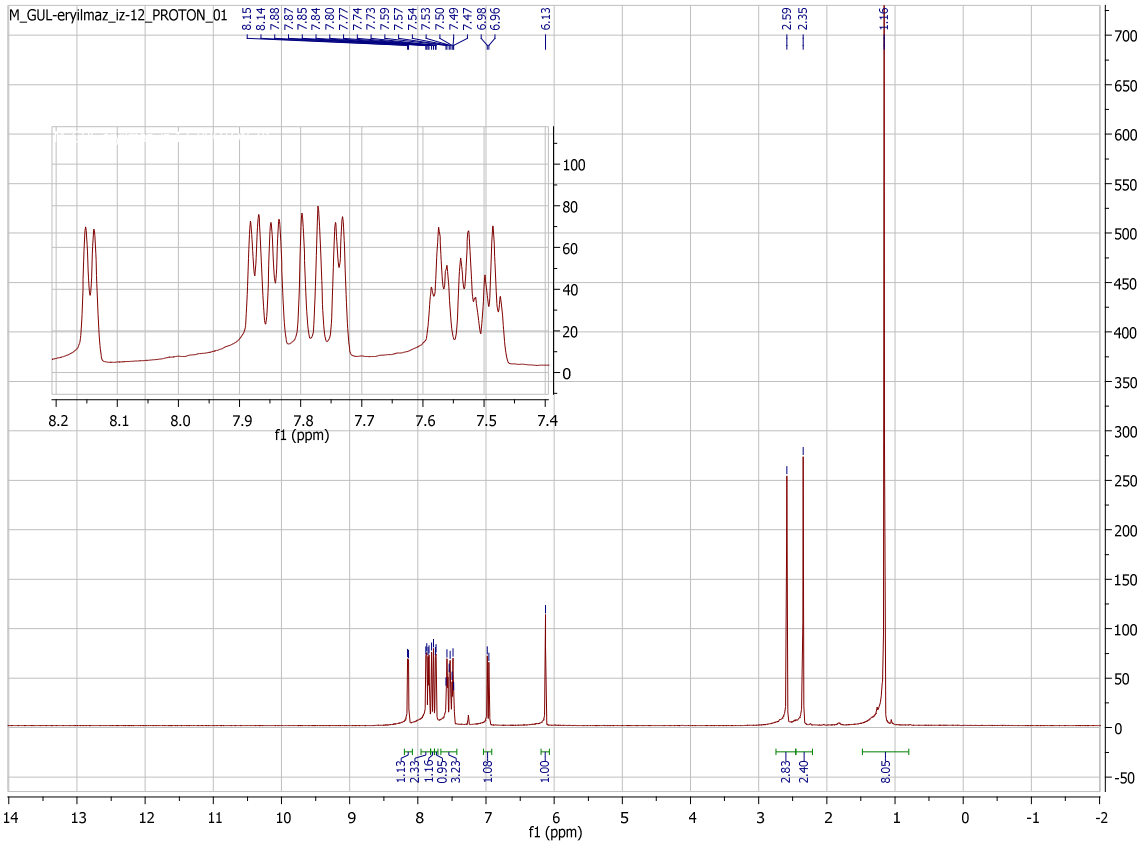

Figure S.3 The ^{1}H-NMR spectrum of the compound I

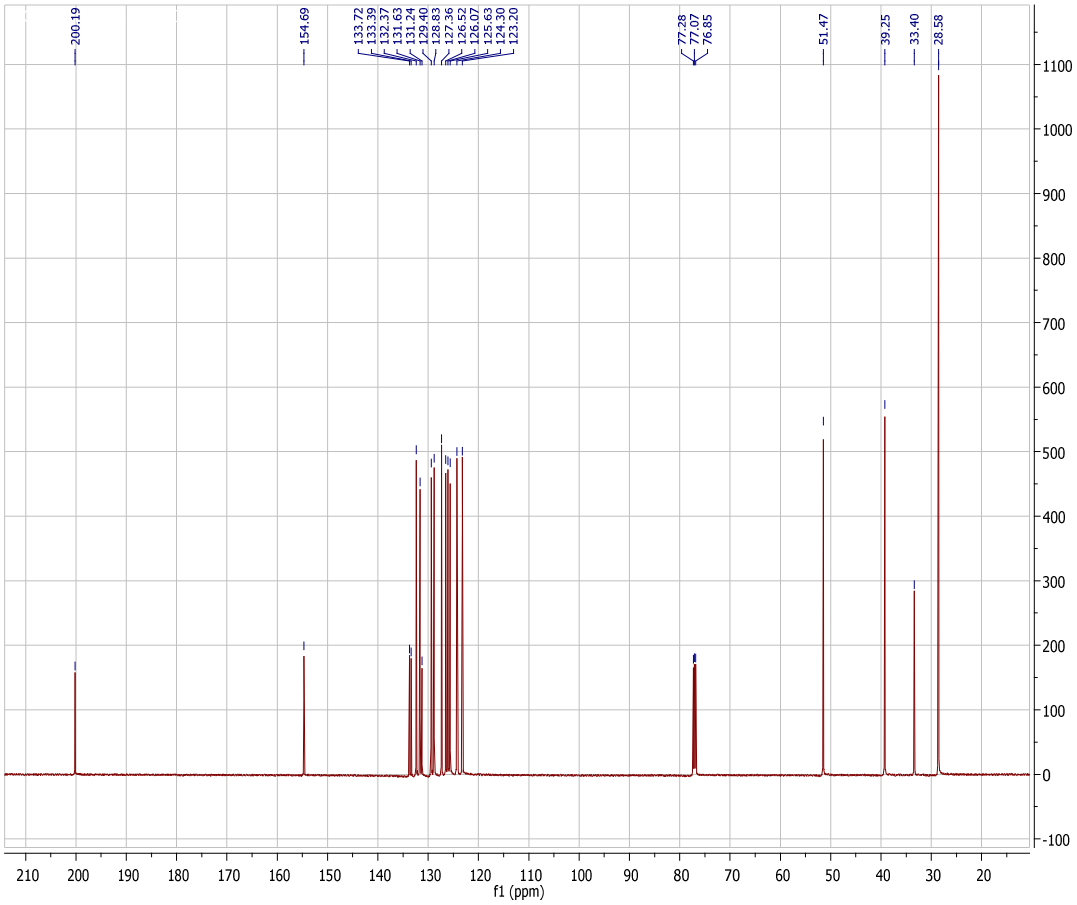

Figure S.4 The ^{13}C-NMR spectrum of the compound I

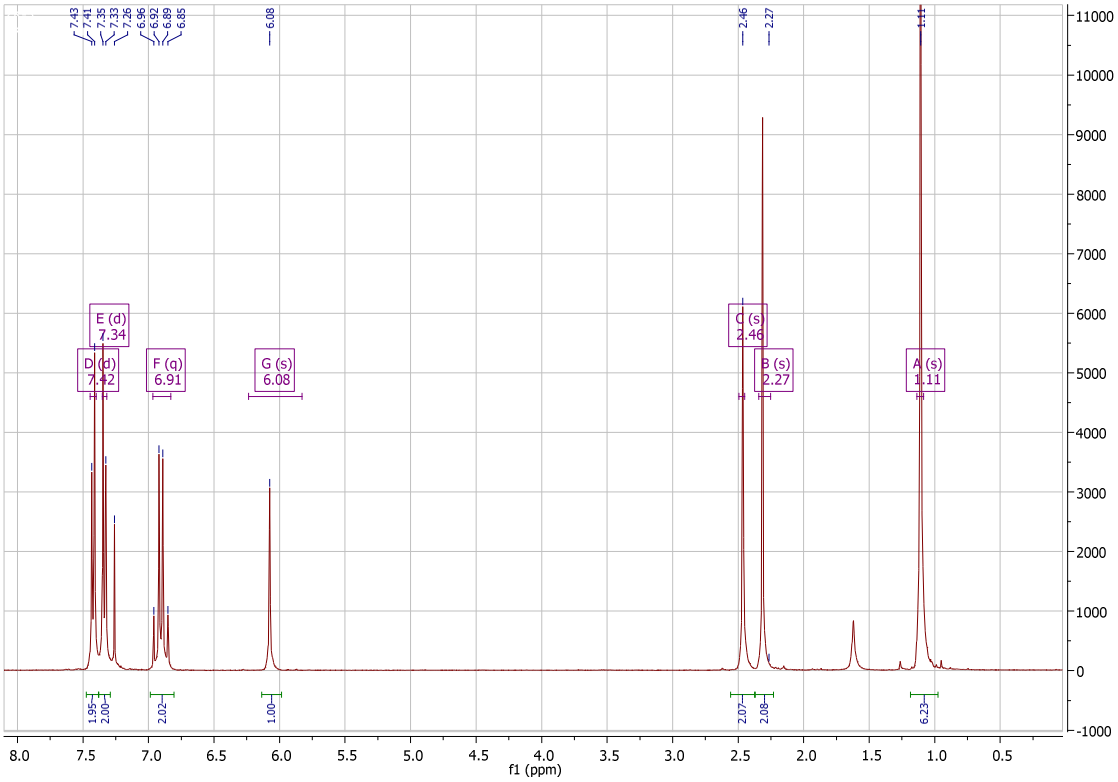

Figure S.5 The ^{1}H-NMR spectrum of the compound II

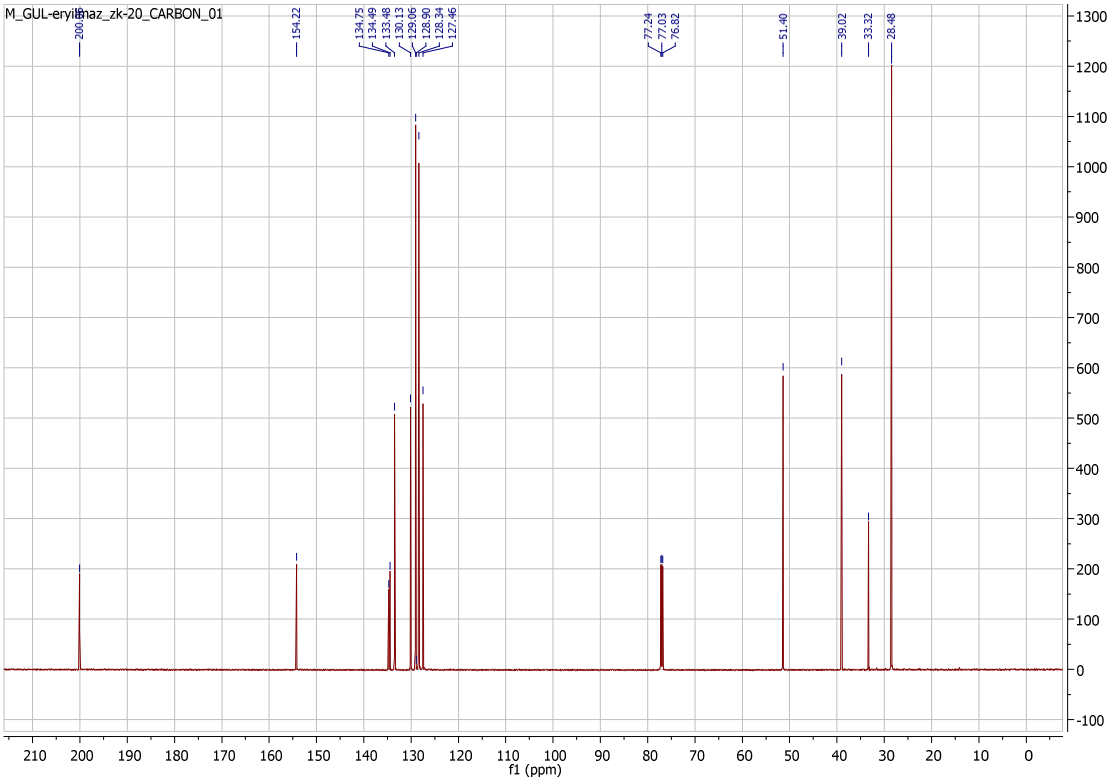

Figure S.6 The ^{13}C-NMR spectrum of the compound II